Multiphase Materials with Lignin. XV. Blends of Cellulose Acetate Butyrate with Lignin Esters

INDRAJIT GHOSH, RAJESH K. JAIN, WOLFGANG G. GLASSER

Biobased Materials/Recycling Center and Department of Wood Science and Forest Products,
Virginia Polytechnic Institute and State University, Blacksburg, Virginia 24061

Received 9 November 1998; accepted 8 March 1999

ABSTRACT: Commercially available cellulose acetate butyrate (CAB, unplasticized) was blended in melt and solution with lignin esters having different ester substituents—acetate (LA), butyrate (LB), hexanoate (LH), and laurate (LL). All lignin esters formed phase-separated blends with CAB with domain size depending on processing conditions and the interaction between phases depending on blend components. CAB/LA and CAB/LB revealed the strongest interactions with domain sizes on the 15–30 nm scale as probed by dynamic mechanical thermal analysis and differential scanning calorimetry. The glass transitions (T_g) followed the Fox equation. Broader transitions corresponding to the T_gs of the two parent components were observed for CAB blends with LH and LL. Transmission electron micrographs revealed differences in the phase dimensions of the blends in accordance with chemical and processing (i.e., melt vs solvent) differences. Modest gains in modulus were observed for low contents (<20 wt %) of LA and LB. © 1999 John Wiley & Sons, Inc. J Appl Polym Sci 74: 448–457, 1999

Key words: multiphase materials; lignin; cellulose acetate butyrate; esters; acetate; butyrate; hexanoate; laurate; dynamic mechanical thermal analysis; transmission electron micrographs; compatibility.

INTRODUCTION

Awareness about the potentially harmful effects of synthetic polymers on the environment has heightened interest in biodegradable materials. These may be based on fermentation-produced, biobased, or otherwise decomposable (in the natural environment) polymeric systems.[1,2] Three main categories of biodegradable polymer systems can be distinguished: (a) natural polymers originating from plant or animal resources (e.g., cellulose, starch, lignin, protein, collagen, etc.); (b) biosynthetic polymers produced by fermentation processes by microorganisms (e.g., polyhydroxy alkanoates); and (c) certain synthetic biodegradable polymers (e.g., polycaprolactone and polylactic acid). Various combinations of biodegradable polymers have been tested for compatibility with conventionally used polymer systems, and these include starch and starch-caprolactone based formulations,[3,4] polycaprolactone and cellulose ester blends,[5] polyhydroxyalkanoate with cellulose esters,[6] and a wide variety of additives.[2] Many natural polymers require chemical modification before they become melt processable,[7–9] and this usually lessens their biodegradability.[10–13]

Lignin, the high modulus amorphous binder of woody plants,[14] is a potential biodegradable additive for polymers of both synthetic and natural origin. Previous studies have revealed that some compatibility exists between modified cellulose and modified lignin. Blend studies on melt-extruded and solvent cast films of hydroxypropyl

---

Correspondence to: W. G. Glasser.

Journal of Applied Polymer Science, Vol. 74, 448–457 (1999)
CCC 0021-8995/99/020448-10

Table I Molecular Weights and Glass Transition Temperature Values

	M_n	M_w	MWD	Mark Houwink Values: A	Mark Houwink Values: Log K	T_g (°C)
CAB 381-20	69,600	127,600	1.83	0.788	−3.808	134
Lignin acetate	1550	5890	3.80	0.204	−2.536	92
Lignin butyrate	2310	7730	3.34	0.218	−2.591	52
Lignin hexanoate	2650	9440	3.56	0.222	−2.585	30
Lignin laurate	13,400[a]	33,200	2.48	0.269	−3.207	2

[a] The unusually large molecular weight may be attributed to poor solubility of the LL derivative in tetrahydrofuran (the solvent used for molecular weight determination), and to the possible formation of solvent-induced aggregates.

cellulose and lignin (L) revealed the presence of secondary interactions between the two components.[15] The lignin component was found to reinforce the amorphous cellulose derivative matrix, which forms an oriented crystal mesophase structure, and this behaves as a nanocomposite structure.[15–17] Further studies were reported on interactions of cellulose and lignin by modifying either or both polymers.[18–20] Many cellulose derivatives, such as ethyl cellulose and cellulose acetate butyrate (CAB), revealed lower compatibility with lignin showing heterogeneous, two-phase morphology both by differential scanning calorimetry (DSC) and scanning electron microscopy over a wide range of compositions.[18,19] Further investigations with the intent of understanding the interaction between liquid crystalline cellulose derivatives and lignin[21] revealed higher degrees of phase mixing for continuous fibers prepared from anisotropic solutions of CAB and L in dimethylacetamide (DMAc). Enhanced miscibility of hemicelluloses and lignin was recognized by Erins et al.[22] and this was attributed to the introduction of carbonyl functionality by acetylation.

This study is aimed at understanding the degree of polymer compatibility between a commercial cellulose ester (CAB) and lignin esters having different ester group substituents (acetate, butyrate, hexanoate, and laurate) using a practical processing techniques. CAB is being used commercially by melt processing for various applications.[7] Modifications with such biodegradable additives as lignin esters may enhance CAB's utility in biodegradable materials as well as reduce cost.

The biodegradability of both lignin and cellulose is self-evident from the fact that wood decays in a variety of biological environments. It also has been widely established that chemical modification harms (retards or prevents) the biodegradability of naturally occurring polymers.[10–13] With cellulose derivatives, it has been observed that, while the introduction of ether groups imposes a virtually insurmountable obstacle to subsequent enzymatic and microbial degradation,[23] esters retard the degradation without preventing it. The extent of retardation thereby seems to be related to the presence vs absence of conditions favoring deacylation.[11] Moisture, pH, temperature, and oxygen are only a few of the parameters influencing the rate of cellulose deacylation and thus biodegradation. Similar effects must be expected for lignin esters, but this deduction by analogy is awaiting experimental verification. The demonstration of biodegradability of the blends described here, if any, therefore needs to be the subject of future studies.

EXPERIMENTAL

Materials

Cellulose acetate butyrate (CAB 381-20) was obtained from Eastman Chemical Company, Kingsport, TN. The average acetyl and butyryl contents were given as 13.5 and 38.1 wt %, respectively, and the falling-ball viscosity was 20 s (76 poise). Other parameters are summarized in Table I. Lignin acetate (LA), lignin butyrate (LB), lignin hexanoate (LH), and lignin laurate (LL) were prepared by esterification of organosolv lignin (L) (Aldrich Chemical Company, WI, Catalog No. 37,101-7) by standard methodology.[24] Pertinent molecular weight data are listed in Table I. All polymers were dried under vacuum at 40°C for 12 h before being blended.

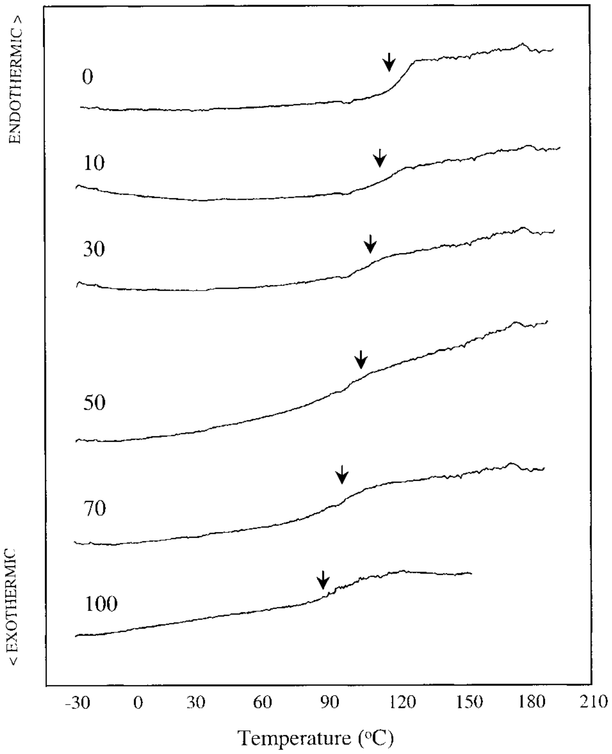

Figure 1 DSC thermograms of solvent ($CHCl_3$) cast samples of CAB and LA. Numbers on each curve denote LA content (wt %) in the blend. These traces are from the second heating scan (after quenching from melt at a rate of 300°C/min).

Methods

Blend Preparation

CAB/lignin ester blends in different proportions were prepared by solvent casting and melt extrusion. For solvent casting, the blend components were stirred in approximately 5 wt % chloroform solution at room temperature before being cast in Teflon molds. The solvent was slowly evaporated at room temperature in a vacuum dessicator (72 h). Any remaining solvent was removed in a vacuum oven at 35°C. For melt-processed blends, corresponding amounts of individual components were physically mixed as powders at room temperature and then transferred to a preheated "Mini-Max Molder" (Custom Scientific Instruments, Whippany, NJ). The polymer was melt mixed at 220°C, with continuous stirring, for approximately 2 min before it was injected into the preheated mold. The cooling rate after injection was not controlled.

Characterization

Thermal analysis was performed on a Perkin-Elmer Model DSC-4 equipped with a Thermal Analysis Data Station using standard aluminum pans. The temperature was scanned from −20 to 180°C at a rate of 10°C/min in nitrogen atmosphere. The T_g was taken as the midpoint of the heat capacity transition ($1/2\Delta C_p$), and it was reported from the second heating scan unless otherwise indicated. Dynamic mechanical properties were determined using a dynamic mechanical thermal analyzer (DMTA) by Polymer Laboratories Ltd., Shropshire, England. Measurements were performed in the single and dual cantilever-bending mode for injection molded samples, and in the shear mode for solvent cast films. The spectra were collected from −20 to 180°C using a heating rate of 4°C/min and a frequency of 1.0 Hz. Mechanical properties were determined on dog-bone specimens using a Miniature Materials Tester (Minimat Model No. SM9-06, by Polymer Laboratories, Loughborough, England). Tests were conducted at room temperature with a 1000 N load beam using strain rates of 5 mm/min. Each reported data point represents the average of four measurements. For transmission electron microscopy (TEM), samples were embedded in Poly/Bed 812 (Polysciences, Inc.) and cured at 60°C for 48 h in flat molds. Sections (80–100 nm thick) were cut from the embedded films with a diamond knife attached to a Reichert Ultracut E microtome and carefully mounted on copper grids. The grids were observed on a JEOL JEM-100CX-II electron microscope operated at an accelerating voltage of 80 kV. The micrographs were from the bright field images of the cut unstained samples at a magnification of 10,000×. Rheological measurements were performed with a Rheometrics RMS-800

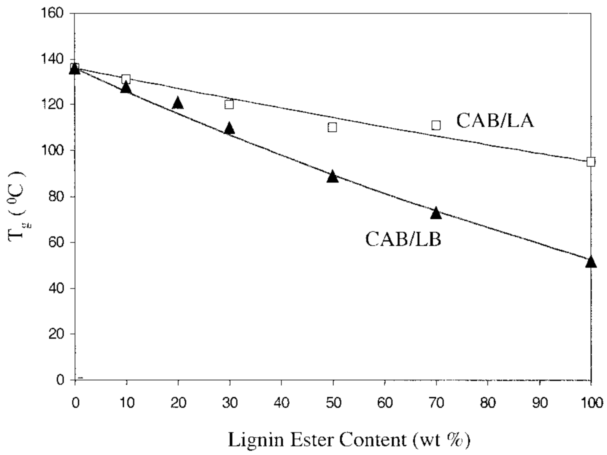

Figure 2 Fox equation fit for blends of CAB/LA and CAB/LB. T_g data obtained from DSC scans.

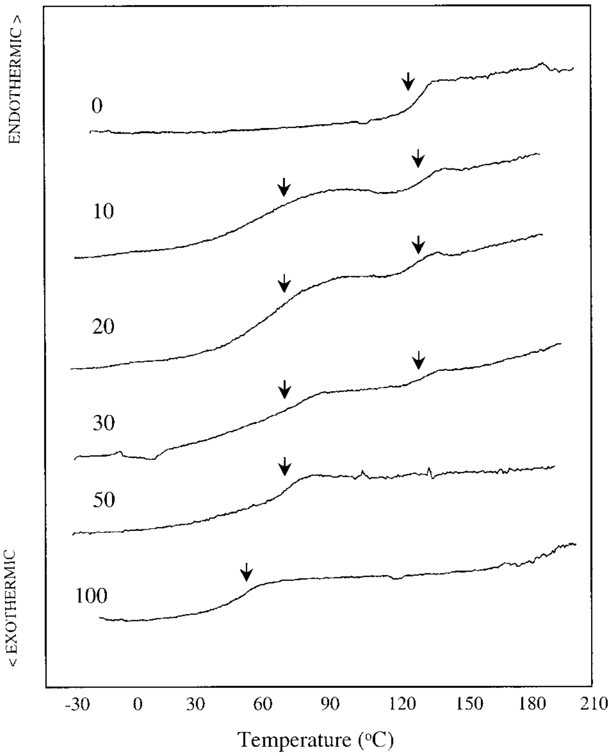

Figure 3 DSC thermograms of solvent ($CHCl_3$) cast samples of CAB and LH. Numbers on each curve denote LH content (wt %) in the blend. These traces are from the first heating scan.

rheometer using 25 mm parallel plates as tooling. The experiments were carried out in the dynamic mode with a maximum of 15% strain in an atmosphere of nitrogen.

RESULTS

DSC Results

The results obtained by DSC reveal single T_gs for all CAB/LA blends (Fig.1). The T_gs shift toward the T_g of LA as LA content increases. The values follow the Fox equation[25] (Fig. 2). Similar results are obtained for CAB/LB blends. However, in all cases the transitions were found to occur over a broader temperature range for blend compositions of 70/30 to 30/70 of CAB/LA or CAB/LB. For CAB/LH blends, distinct second-order transitions corresponding to the T_gs of the parent components were observed in the first heating scan (Fig. 3). The lower transition thereby is found to correspond to the T_g of LH, whereas the transition at the higher temperature is assigned to CAB. Both transitions occur at almost the same temperature as that of the parent, and both failed to shift much with composition. However, the transition corresponding to CAB becomes weaker as the amount of LH increases, and it ultimately becomes undetectable at a 50% blend composition. In the second heating scans, only single transitions were observed for all blends, and these are broader and less well distinguished. This disappearance of T_g transitions in lignin during repeated heating has been noted before, and it suggests some sort of reorganization in the rubbery state. The T_gs (first heating scan) of the CAB/LH blends do not follow the Fox equation (Fig. 4). DSC results for CAB/LL blends were all similar to those of the CAB/LH blends.

DMTA Results

DMTA measurements of CAB/LA blends reveal a shift in the modulus curves (E' and E'') toward lower temperatures as the amount of LA increases in the blends (Fig. 5). Similarly, the tan δ peaks also shift toward lower temperatures as LA content increases (Fig. 6). However, all compositions of the CAB/LA blends are represented by tan δ and log E'' curves that indicate single T_gs only. If the T_g values are taken as the points of inflexion of the loss modulus curves (where the curve changes from convex to concave or reverse, i.e., derivative of the slope of the curve is zero), the data correspond to the DSC results and follow the Fox equation (Fig. 2). Similar to DSC results, the tan δ peaks broaden as the LA content increases.

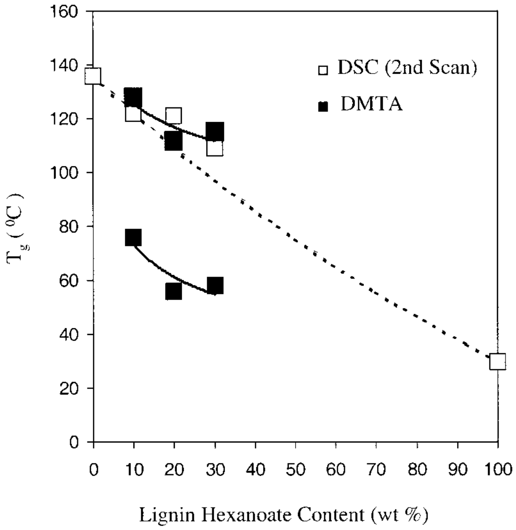

Figure 4 Fox equation fit for blends of CAB and LH.

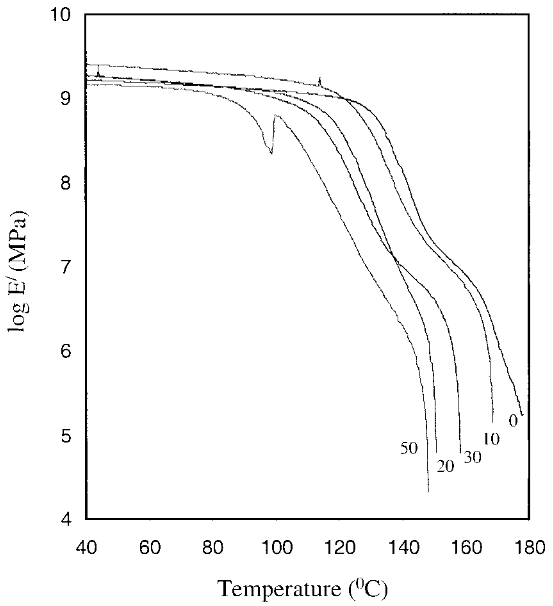

Figure 5 Storage modulus vs temperature curves for blends of CAB and LA obtained from DMTA experiments at 1 Hz. The loss modulus (E'') showed analogous behavior. Numbers on each curve denote LA content (wt %) in the blend.

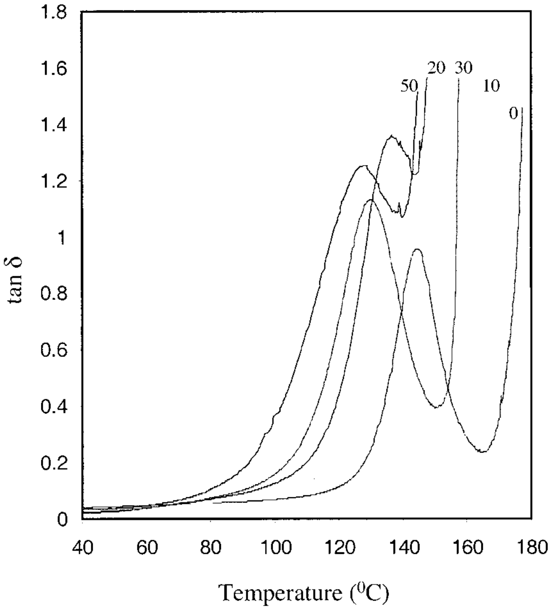

Figure 6 Tan δ vs temperature curves for blends of CAB and LA obtained from DMTA experiments at 1 Hz. Numbers on each curve denote LA content (wt %) in the blend.

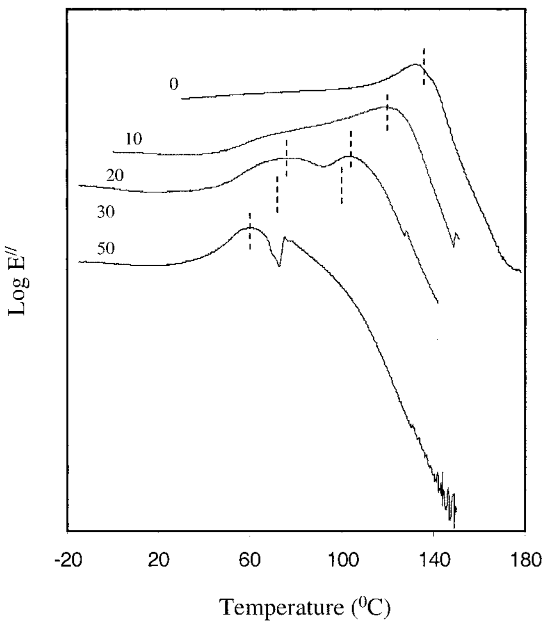

Figure 7 Loss modulus vs temperature curves for blends of CAB and LH obtained from DMTA experiments at 1 Hz. Curves have been shifted on the modulus axis for greater clarity. Numbers on each curve denote LH content (wt %) in the blend.

Similarly, for CAB/LB blends, all compositions are described by modulus shifts toward lower temperatures as well as by single tan δ and loss modulus (log E'') peaks (not shown). The T_gs represented by the points of inflexion of the loss modulus curves are comparable to the T_gs obtained by DSC and they follow the Fox equation (Fig. 2). However, the decrease in the log E' curves occurs over a wider temperature range (and the modulus flattens out) as the LB content increases in the blends. This behavior is pronounced only in the case of CAB/LB blends and not in others. Since this behavior resembles cold crystallization of polymers, where the modulus remains constant or even increases after the rising temperature passes through T_g, it might be suspected that the LB component contributes to some sort of molecular reorganization in CAB. Such an effect by lignin (derivatives) on the organizational behavior of cellulose derivatives has been noted before.[16,17,19,20]

In case of melt-processed CAB/LH blends, however, an emergence of a second peak corresponding to the LH component is observed in the loss modulus (log E'') curves obtained by DMTA analysis in the bending mode (Fig. 7). The log E'' transition gradually separates into two as the LH content rises above 10%. The tan δ peaks for these melt-processed blends, however, reveal single transitions, which shift toward lower tempera-

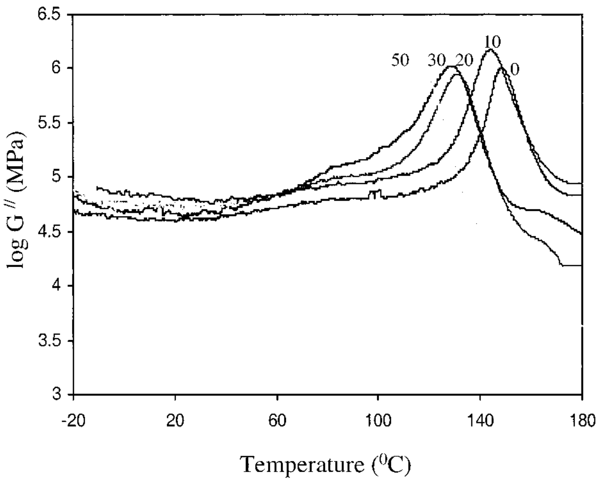

Figure 8 Loss modulus vs temperature curves for solvent cast blends of CAB and LH obtained from DMTA experiments at 1 Hz in shear mode. Numbers on each curve denote LH content (wt %) in the blend.

tures (except in the case of the highest LH content where a shoulder is found near 80°C). The DMTA results for solvent cast films of CAB/LH also reveal the emergence of a lower temperature transition (Fig. 8). The transitions, as shown by the loss modulus curves, are found to occur over a wide temperature range in the blends with high LH contents. Similar results were obtained for CAB/LL blends (not shown).

TEM Results

Transmission electron micrographs of solvent cast blends of CAB with 20 and 50 wt % LH clearly indicate differences in the size of the LH phases dispersed within the continuous CAB phase (Fig. 9a, b). The darker phase represents the lignin component due to the higher electron density in the phenyl rings (i.e., presence of conjugated π electrons). A comparison between the solvent cast and melt blended samples of 20%

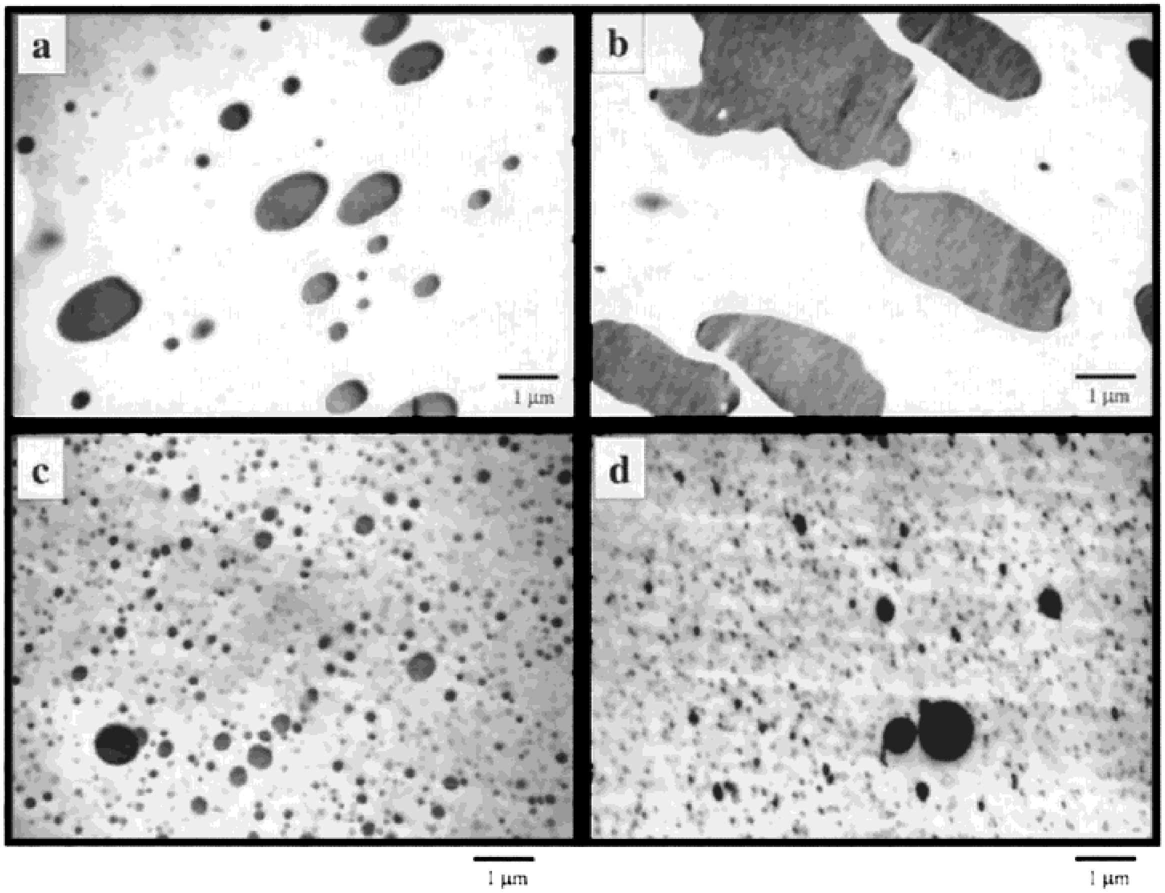

Figure 9 Transmission electron micrographs of CAB/lignin-ester blends with (a) solvent cast 20% LH; (b) solvent cast 50% LH; (c) melt blended 20% LH; (d) melt blended 20% LA by weight (magnification at 10,000×).

LH/CAB reveals a better dispersion of the LH phase when melt blended compared to solvent casting (Fig. 9a,c). The mean domain sizes (obtained by averaging the domain sizes of the lignin ester phases within a square inch cross-sectional area of the transmission electron micrographs) of CAB/LH blends for solvent casting is 1000 nm as compared to 170 nm for melt blended samples. Either these results can be explained with a thermodynamically or a kinetically controlled process of phase formation, or they may be viewed as the formation of an unstable system subject to change during aging. Considering solvent casting as an equilibrium process, lignin ester molecules can be expected to aggregate together to obtain the lowest possible energy configurations and form larger domains. Melt blending, by contrast, can be expected to favor greater dispersion of the lignin ester molecules in the CAB phase owing to the high shear forces applied during mixing as well as the high rate of subsequent cooling from the melt, which represents a nonequilibrium process. The results, however, are also consistent with the view that the solvent cast samples have a morphology that reflects an unstable mixture formed by a rapidly changing ternary phase diagram (solvent–CAB–lignin) in which the miscibility (or nonmiscibility) of the CAB–lignin mixture is determined as a function of the precise position on this diagram as the solvent is removed. The resulting morphology would, in this case, change with aging above the T_g. In any event, the domain sizes of the lignin ester phases are smaller in case of melt blending as compared to solvent casting. This is consistent with a kinetically as opposed to thermodynamically controlled process. Melt processing using different shear rates during mixing can be expected to produce materials with different morphologies.

The term "polymer compatibility" is much used but ill-defined. It usually refers to the degree of the interaction between polymer pairs at the molecular level. Since mixing of molecules is ruled out on thermodynamic grounds, the compatibility can only be defined in relative terms of the dimensions of separate and distinct phases. These dimensions are generally characterized by such measurement techniques as DSC, DMTA, thermomechanical analysis, NMR, etc. The detection of a single or double transition in a two-phase system by an instrument gives an indication of the dimensions of the phases present in the system. Using the compatibility concept of Kaplan,[26] phase dimensions can be estimated. The dimension that corresponds to a DMTA transition is approximately 15–30 nm,[26] NMR distinguishes fluctuations in the range of 2.5–5 nm,[27] and DSC has an estimated resolution of 100–500 nm. Since the results observed by DSC and DMTA with CAB/LA and CAB/LB blends show single T_gs for all compositions, with T_g following the Fox equation, compatibility at the 30–100 nm scale is indicated. TEM also provides evidence in support of phase dimensions in the range of 10–100 nm for melt blended samples of CAB/LA (Fig. 9). However, blends with LH and LL reveal two distinct T_gs by both DSC (in first heating scan) and DMTA. This suggests phase dimensions of >150 nm. This is also evident from the results of TEM, where phase dimensions in the range of 75–500 nm are indicated (Fig. 9c). Therefore, as the size of the substituent in lignin esters increases, blends proceed from "compatible" to "semicompatible." This change is also reflected by the mechanical properties. Similarly, peculiar and enhanced interactions between CAB and Novolac (phenolic prepolymer) were also observed by Davis et al.,[28] who attributed the behavior to the formation of H bonds between the butyryl and the phenolic OH groups. However, in case of CAB/lignin esters, the phenolic OH functionality could not have been responsible for the interaction between CAB and LA, which is a nonphenolic derivative.

Mechanical Properties

(Isolated) lignin and lignin esters are small molecules ($M_n \approx 10^3$) compared to the much larger CAB ($M_n \approx 10^5$) that is dispersed in the CAB continuous phase. Since the discontinuous phase (i.e., lignin) is in the glassy state, this combination acts as a nanocomposite with the lignin component serving as reinforcing filler for the CAB phase. Lignin, therefore, can be expected to enhance the modulus of the continuous phase. This effect is indeed revealed by the mechanical property analysis of the blends at room temperature (Figs.10–12). Whereas tensile strength and elongation at break consistently decline with lignin derivative content (Figs.10 and 11) modulus increases for both the CAB blends with LA and LB (Fig.12). In the case of CAB/LA, a 10% increase in modulus is observed for 10% incorporation of LA (Fig.12), and CAB/LB reveals a modulus increase of more than 20% with LB content rising to 20 wt %. A molecular (discussed earlier) or more favorable interaction of LB with CAB owing to a higher butyryl as compared to acetyl content in CAB may

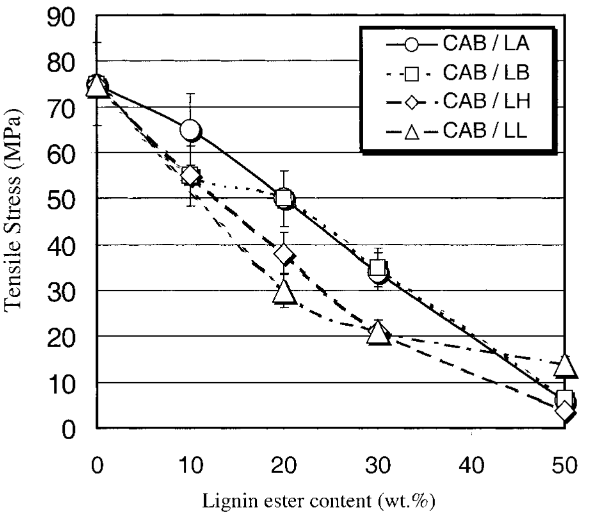

Figure 10 Tensile stress vs lignin ester content for CAB/lignin ester blends.

account for this difference between LA and LB. Therefore, LB is a better modulus builder for CAB than LA, and the optimum lies around 20 wt % LB. Whereas the modulus does not change when LH content rises to 20%, LL seems to serve as CAB plasticizer at room temperature. This was expected since LL has a T_g below room temperature.

Rheological Characterization

Melt viscosity measurements were carried out at three temperatures (200, 220, and 240°C) using CAB and two CAB/LA blends having a 10 and 20% LA content. The relationship between complex viscosity (η^*) and frequency (ω) at 200°C reveals that the viscosity of the CAB/LA blends is always greater than the viscosity of pure CAB (Fig.13). This was found to be consistent at all temperatures of measurement. However, the relative amount of LA had no noticeable influence on the viscosity vs. frequency relationship (Fig.13). The viscosity-raising effect of lignin had been reported earlier for blends with polypropylene.[29] The decrease in shear stress (i.e., increase in viscosity) at constant shear rate for polypropylene–lignin blends had been attributed to increased

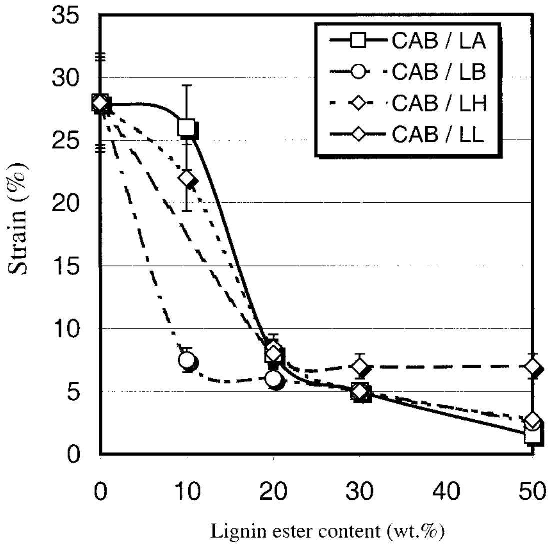

Figure 11 Strain (at break) vs lignin ester content for melt blended samples of CAB/lignin ester.

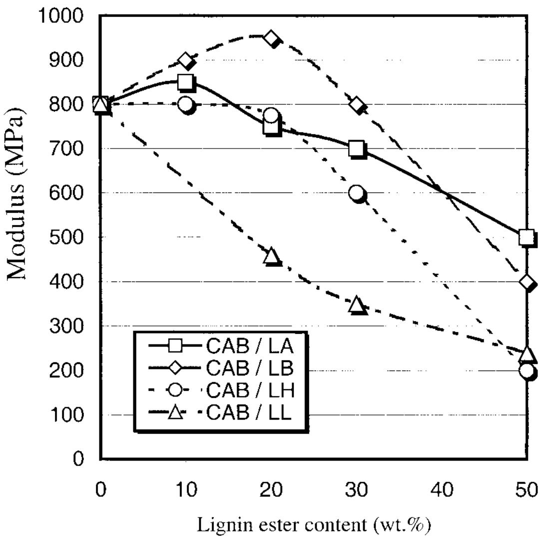

Figure 12 Modulus vs lignin ester content for melt blended samples of CAB/lignin ester.

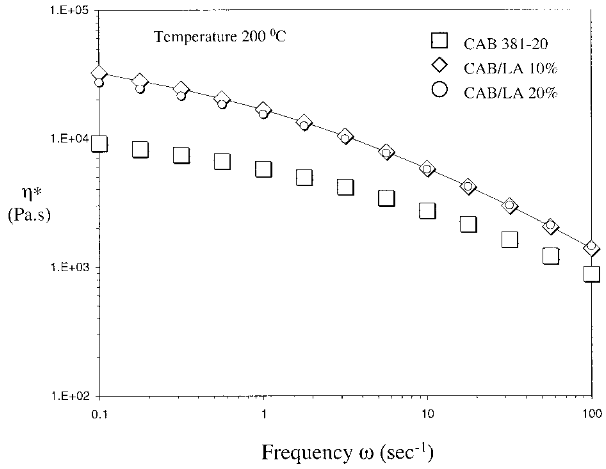

Figure 13 Viscosity data for different blends of CAB/LA at 200°C.

crosslinking.[29] However, in case of CAB/LA blends, LA acts as an antiplasticizer for CAB by reducing T_g and raising the modulus of the blend system. Crosslinking can be ruled out since the hydroxyl groups of lignin have been replaced by ester substituents. There has been no evidence to suggest that lignin undergoes crosslinking or transesterification with CAB. By contrast, however, it is the observed significant phase interaction between CAB and lignin esters (especially LA and LB) that must be held responsible for the increase in viscosity when lignin ester is added to the melt.

CONCLUSIONS

1. The blends of CAB and lignin esters are phase separated with domain sizes depending upon processing conditions and the interaction between phases depending upon blend composition.
2. The CAB/LA and CAB/LB blends reveal single T_gs for all compositions by both DSC and DMTA. The transitions follow the Fox equation and hence are compatible on the 30–150 nm scale.
3. CAB/LH and CAB/LL blends form two distinct transitions (or broader transitions) corresponding to the T_gs of CAB and LH or LL.
4. TEM results reveal phase dimensions of the lignin ester phases, which are in accordance with the results of other measurements. A transition from full compatibility to semicompatibility is observed for the CAB/lignin esters blends as the ester substituent increases from two to twelve carbon atoms.
5. The T_gs decrease with the incorporation of any of the lignin esters, and the lignin esters act as polymeric plasticizers for CAB.
6. The phase dimensions (from TEM results) for solvent cast blends are greater than those for melt blended samples.
7. Modulus increases are observed in cases of CAB blends with LA and LB but not for CAB/LH or CAB/LL. Tensile strength and ultimate strain decrease in all blends.
8. The complex viscosity of CAB increases with the addition of LA and this suggests strong phase interactions.
9. Short-chain lignin esters (acetate and butyrate) can be used as polymeric plasticizers as well as modulus builders for commercial CAB.

The authors wish to express gratitude to the Eastman Chemical Company for the supply of CAB and to Prof. D. G. Baird and Dr. Mike McLeod, Department of Chemical Engineering, Virginia Tech, for assistance with the viscosity measurements. The authors also thank an anonymous reviewer for making constructive suggestions, which contributed to significant improvements of an earlier version of this article.

REFERENCES

1. Swift, G. In "Agricultural and Synthetic Polymers-Biodegradability and Utilization." Glass, J. E., Swift, G., Eds.; American Chemical Society Press, Washington, DC, ACS Symp. Ser. No. 433, 1990; pp 2–12.
2. Kaplan, D. L.; Mayer, J. M.; Ball, D.; McCassie, J.; Allen, A. L.; Stenhouse, P. In "Biodegradable Polymers and Packaging." Ching, C., Kaplan, D. L., Thomas, E. L., Eds.; Technomic Publishers, Lancaster, 1993; pp 1–42.
3. Griffin, G. J. L. In "Fillers and Reinforcements for Plastics." R. D. Deanin and N. R. Scholt, eds. American Chemical Society, Washington, DC. Adv. Chem. Ser. No. 134, 1974, p 159–170.
4. Narayan, R.; Bloembergen, S. Polym Prepr 1990, 32(2), 119.
5. Nishio, Y.; Matsuda, K.; Miyashita, Y.; Kimura, N.; Suzuki, H. Cellulose 1997, 4, 131.
6. Lotti, N.; Scandola, M. Polym Bull 1992, 29, 407.
7. Bogan, R. T.; Brewer, R. J. In "Cellulose Esters, Plastics," Encyclopedia of Polymer Science and Engineering, J. I. Kroschwitz, ed. John Wiley & Sons: New York, 1985; Vol 3, pp 181–200.
8. Serad, G. A. In "Cellulose Esters, Fibers," Encyclopedia of Polymer Science and Engineering; J. I. Kroschwitz, ed. John Wiley & Sons: New York, 1985; Vol 3, pp 200–226.
9. Maddever, W. J.; Campbell, P. D. In "Degradable Materials: Perspectives, Issues and Opportunities" S. A. Barengerg; J. L. Brash; R. Narayan, A. E. Redpath, Eds.; CRC: Boston, 1990; 237–262.
10. Reese, E. T. Ind Eng Chem 1957, 49, 89.
11. Buchanan, C. M.; Gardner, R. M.; Komarek, R. J. J Appl Polym Sci 1993, 47, 1709.
12. Glasser, W. G.; McCartney, B. K.; Samaranayake, G. Biotechnol Prog 1994, 10, 214.
13. Glasser, W. G.; Ravindran, G.; Jain, R. K.; Samaranayake, G.; Todd, J. Biotechnol Prog 1995, 11, 552.
14. Glasser, W. G.; Kelley, S. S. In "Lignin" Encyclopedia of Polymer Science and Engineering, 2nd ed.; J. I. Kroschwitz, ed. John Wiley & Sons: New York, 1987; Vol. 8, pp 795–852.
15. Rials, T. G.; Glasser, W. G. J Appl Polym Sci 1989, 37, 2399.
16. Dave, V.; Glasser, W. G.; Wilkes, G. L. Polym Bull 1992, 29, 565.

17. Glasser, W. G.; Rials, T. G.; Kelley, S. S.; Dave, V. In "Cellulose Derivatives—Modification, Characterization, and Nanostructure." Heinze, T. J., Glasser, W. G., Eds.; ACS Symposium Series No. 688; American Chemical Society: Washington, DC, 1998; p 265.
18. Rials, T. G.; Glasser, W. G. Polymer 1990, 31, 1333.
19. Rials, T. G.; Glasser, W. G. Wood and Fiber Science 1989, 21(1), 80.
20. Rials, T. G.; Glasser, W. G. In "Lignin—Properties and Materials," Glasser, W. G., Sarkanen, S. Eds.; American Chemical Society: Washington, DC, ACS Symp. Ser. No. 397, 1989, pp 464–475.
21. Dave, V.; Glasser, W. G. Polymer 1997, 38(9), 2121.
22. Erins, P.; Cinite, V.; Jakobsons, M.; Gravitis, J. J Appl Polym Sci, Appl Polym Symp No 28(3), 1976, 1117.
23. Just, E. K.; Majewicz, T. G. In "Cellulose Ethers," Encyclopedia of Polymer Science and Engineering, 2nd ed.; J. I. Kroschwitz, ed. John Wiley & Sons: New York, 1987; Vol 3, pp 226–269.
24. Glasser, W. G.; Jain, R. K. Holzforschung 1993, 47(3), 225.
25. Fox, T. G., Bull Am Phys Soc 1956, 2(2), 123.
26. Kaplan, D. S. J Appl Polym Sci 1976, 20, 2615.
27. Masson, J. F.; St. John Manley, R. Macromolecules 1992, 25, 589.
28. Davis, M. F.; Wang, X. M.; Myers, M. D.; Iwamiya, J. H.; Kelley, S. S. In "Cellulose Derivatives—Modification, Characterization, and Nanostructure"; Heinze, T. J., Glasser, W. G., Eds.; ACS Symposium Series, No. 688; American Chemical Society: Washington, DC, 1998; 283.
29. Kosikova, B.; Demianova, V.; Kacurakova, M. J Appl Polym Sci 1993, 47, 1065.